

## Computational estimation of ms-sec atomistic folding times

Upendra Adhikari<sup>†</sup>, Barmak Mostofian<sup>†</sup>, Andrew Petersen<sup>‡</sup>, and Daniel M. Zuckerman<sup>†\*</sup>

<sup>†</sup>*Department of Biomedical Engineering, School of Medicine, Oregon Health & Science University, Portland, OR 97219*

<sup>‡</sup>*NCSU Data Science Resources, North Carolina State University, Raleigh, NC 27695*

\* [zuckermd@ohsu.edu](mailto:zuckermd@ohsu.edu)

Despite the development of massively parallel computing hardware including inexpensive graphics processing units (GPUs), it has remained infeasible to simulate the folding of atomistic proteins at room temperature using conventional molecular dynamics (MD) beyond the  $\mu$ s scale. Here we report the folding of atomistic, implicitly solvated protein systems with folding times  $\tau_f$  ranging from  $\sim 100 \mu$ s to  $\sim 10$ s using the weighted ensemble (WE) strategy in combination with GPU computing. Starting from an initial structure or set of structures, WE organizes an ensemble of GPU-accelerated MD trajectory segments via intermittent pruning and replication events to generate statistically unbiased estimates of rate constants for rare events such as folding; no biasing forces are used. Although the variance among atomistic WE folding runs is significant, multiple independent runs are used to reduce and quantify statistical uncertainty. Three systems were examined: NTL9 at low solvent viscosity (yielding  $\tau_f \sim 5 \mu$ s), NTL9 at water-like viscosity ( $\tau_f \sim 40 \mu$ s), and Protein G at low viscosity ( $\tau_f \sim 10$ s). In all cases the folding time, uncertainty, and ensemble properties could be estimated from WE simulation; for protein G, this characterization required significantly less overall computing than would be required to observe a *single folding event* with conventional MD simulations. Our results suggest discrepancies with experimental folding times that should enable improvement of force fields and solvent models.

## Introduction

Elucidating the kinetics and mechanisms of protein folding has been a decades-long focus of molecular biophysics, both experimental and theoretical/computational.<sup>1-19</sup> Significant challenges remain, however, notably whether molecular dynamics (MD) simulations will provide the hoped-for reproducible and atomically detailed folding trajectories.<sup>1, 11, 13-14, 20-23</sup> Despite isolated reports of success,<sup>24</sup> MD simulations generally have not produced *room temperature* atomistic folding trajectories beyond the  $\mu\text{s}$  timescale even with modern hardware.<sup>25</sup> Promising results have been reported using path-sampling techniques<sup>26-30</sup> but no simulation methodology has emerged as a general-purpose tool for folding, especially for timescales beyond the  $\mu\text{s}$  range.

Here we report substantial progress in the application of the weighted ensemble (WE) path sampling method<sup>31-35</sup> to room-temperature folding at the ms and sec scales, exploiting the power of GPU and cluster computing. We study three atomistic implicitly solvated systems: NTL9 with low and high-friction solvent, as well as Protein G at low friction. These are costly studies, requiring aggregate trajectory totals of 10s to 100s of  $\mu\text{s}$  per system, but they enable fairly precise (order-of-magnitude) estimation of folding rate constants. In earlier work, Ensign and Pande<sup>25</sup> were able to estimate the WW-domain folding time of  $\sim 100 \mu\text{s}$  at room temperature using distributed computing with a total cost of 400 – 500  $\mu\text{s}$  per system. To our knowledge, there are no other reports of room-temperature atomistic protein folding at the ms scale and beyond. Prior folding studies of NTL9 and Protein G were conducted at high temperature (355 K<sup>1</sup>/370 K<sup>36</sup>, and 350 K<sup>1</sup> respectively) because of the prohibitive room-temperature timescales.

In addition to information about protein folding, the ability to quantify rate constants for slow-timescale biomolecular behavior is a critical step in model (force field) development. Although MD simulation is now a standard tool in structural biology studies,<sup>37-40</sup> the governing parameters of MD force fields have been determined based on energy minima<sup>41-45</sup> whereas energy barriers are expected to govern kinetic behavior. Given the evident importance of dynamic biomolecular phenomena, it is critical to obtain simulation-based rate constants to permit further refinement of force fields. However, force fields cannot be assessed fully without the ability to compute kinetic observables, and we report on significant progress in this regard.

The WE method employed in the present report is one of a number of path sampling approaches based on rigorous statistical mechanics<sup>32, 46-51</sup> capable of yielding unbiased rate constants. Although all these methods are theoretically well-grounded, WE does offer the pragmatic advantage of being fully independent of the dynamics engine employed, which has enabled its application with a wide range of both molecular and cell-scale simulation

software.<sup>33, 52-58</sup> This versatility facilitated the integration of the WESTPA software package<sup>59</sup> with the GPU-accelerated version of the AMBER molecular dynamics package<sup>60-62</sup> as employed here. The WE method yields ensembles of fully continuous trajectories from which non-equilibrium observables can be calculated, including kinetic and mechanistic properties.

## Results

The WE procedure takes advantage of running in parallel multiple simulations with well-defined probabilities (or weights) in a conformational space that typically is divided based on pre-defined progress coordinates (see Fig. 1A).<sup>31</sup> The trajectory pruning and replication strategy facilitates progress along the coordinates and guarantees a constant total weight of all trajectories during the WE simulation (see SI Methods for more details). Fig. 1B shows a comparison of a brute-force MD simulation with a typical WE simulation, both starting from the same unfolded NTL9 structure. After  $\sim 7 \mu\text{s}$  of aggregate simulation time, the NTL9 C $\alpha$ -RMSD in the MD simulation remains  $> 6 \text{ \AA}$ , whereas in the WE simulation folded NTL9 structures with C $\alpha$ -RMSD  $< 1 \text{ \AA}$  are sampled. The probability flux of simulations reaching the target state allows estimation of the folding kinetics and the interrogation of continuous trajectories can provide information on folding mechanisms.

The data in Figs. 2-4 show that the probability flux into the folded states, which is an estimator for the rate constant,<sup>63</sup> reaches a steady value in all three atomistic folding systems: NTL9 at low friction, NTL9 at high friction, and Protein G at low friction. The steady values indicate the systems have relaxed into steady states as a function of elapsed molecular time and that errors in estimating the force field specific folding rate constants for the given starting structure are governed by statistical noise. Note that although the average rate constant is dominated by a relatively small fraction of runs, the dominating runs switch during the course of the trajectories (Figs. S1-S3). The “molecular time”,  $t_{\text{mol}}$ , shown in Figs. 2-4 represents the time elapsed during individual trajectories. WE uses an ensemble of trajectories which all require computing resources, and aggregate simulation times are given in Table 1 (see SI for WE parameters and computing resources). Additional runs for the NTL9 systems were performed with alternative WE protocols to confirm the consistent, unbiased nature of the data: Figs. S4 and S5 show consistent time evolution of the folding flux for both low and high-friction systems.

The present study necessarily estimated folding times specific to the chosen force field and solvent model, and also conditioned on the starting structures. The novelty of the results is their relatively high precision and unbiased nature due to the theoretical foundations of the WE method.<sup>34</sup> Hence, although comparison to experimental folding times are shown in Table 1, readers are cautioned that the present study should be considered a first step in assessment of molecular models and initial ensembles. Given these caveats, the rough agreement with

experimental values is encouraging but also points to the need for further investigation of solvent modeling and initial ensembles as discussed below.

A comparison of the folding times (specific for the force field) and the aggregate simulation times as given in Table 1 also enables assessment of the effectiveness of the WE protocol. In the case where WE exhibits least enhancement of sampling, namely NTL9 at low friction (Fig. 2), the force field specific folding time of  $\sim 5\mu\text{s}$  employed  $\sim 100\mu\text{s}$  of aggregate simulation. Fig. 2 reveals that much of the computation was used to confirm steady-state behavior and in fact the folding time could have been inferred from substantially less computation. In principle, similar results could have been obtained via 5-10 independent standard MD runs totaling the same aggregate simulation time. However, given the experimental ms folding time, it is unlikely such MD runs would have been attempted, and WE provided a reliable estimate in an affordable amount of computing effort. The higher-friction NTL9 study, which should be a better mimic of aqueous viscosity,<sup>64-66</sup> reveals a folding time of  $\sim 40\mu\text{s}$  (Fig. 3) that is essentially prohibitive for harvesting multiple events via conventional MD, even on modern GPU platforms. The value of the WE protocol is unambiguous for the slower Protein G system, where a  $\sim 10\text{ s}$  folding time is estimated in much less than a ms of aggregate simulation time (Fig. 4). By comparison, the computational cost of rate estimation here is significantly less than the previously reported overall cost of  $\sim 500\mu\text{s}$  to estimate a  $\sim 65\mu\text{s}$  room-temperature folding time.<sup>25</sup>

During the WE process, a variety of folding trajectories are simulated, enabling unbiased computation of ensemble properties. The weighted distributions of  $\text{C}\alpha$ -RMSD values shown in Figs. S6A, S7A for the NTL9 simulations and in Fig. S8A for the Protein G simulation serve as effective folding free energy profiles, which indicate that NTL9 folding has an energy minimum at  $\text{C}\alpha$ -RMSD =  $\sim 6\text{ \AA}$  and Protein G at  $\text{C}\alpha$ -RMSD =  $\sim 10\text{ \AA}$ . These regions are separated from the folded state by a free energy barrier, suggesting a definition of the transition region and thus allowing calculation of the transition times (event durations) of the continuous WE folding trajectories. Of growing interest,<sup>67-68</sup> the event duration depends on the exact event starting point and on the solvent viscosity.<sup>69-70</sup> For NTL9, at low viscosity, the distributions of event duration have a peak at 1.5 - 2 ns (Fig. S6B), while at the higher water-like viscosity the peaks occur at slightly larger values  $\sim 4$ -5 ns (Fig. S7B). For Protein G, the event duration peaks are less clearly defined but occur in the range of  $\sim 2$ -7 ns (Fig. S8B).

A visual analysis of representative intermediate structures sheds light on the folding mechanisms. The NTL9 molecular structures shown in Fig. 5A illustrate that during the folding process the  $\alpha$ -helix is formed first, followed by the formation of the N-terminal  $\beta$ -hairpin. A putative rate-limiting step of NTL9 folding is characterized by the association of the C-terminal  $\beta$ -strand with the N-terminal  $\beta$ -hairpin through hydrogen bonds. During the final steps ( $1\text{ \AA} < \text{C}\alpha$ -RMSD  $< 4\text{ \AA}$ ), the protein reduces its solvent-accessible surface area by  $\sim 5\text{ nm}^2$  when

forming the remaining native hydrogen bonds, bending the N-terminal  $\beta$ -hairpin turn, and aligning the  $\alpha$ -helix with the  $\beta$ -sheet. Similarly, Protein G (Fig. 5B) folds by first forming the  $\alpha$ -helix and both  $\beta$ -hairpins and then bringing them all closer to each other, which appears to define the main free energy barrier, before connecting the two hairpins with hydrogen bonds and establishing the 4-stranded  $\beta$ -sheet. From the initial formation of the secondary structural elements to the fully folded structure (i.e.  $1 \text{ \AA} < C\alpha\text{-RMSD} < 10 \text{ \AA}$ ), Protein G reduces its overall surface area by  $\sim 8\text{nm}^2$ .

## Discussion

The data reported here suggest that molecular dynamics calculations may soon be able to measure precisely and regularly a broad array of experimentally relevant timescales characterizing functional motions of biomolecules. Such measurements are necessarily limited by the accuracy of the underlying model equations (i.e., the force field) but understanding and correcting force field mis-calibrations is essential for progress in computational structural biology. These corrections will not be possible without reliable kinetics measurements, and the present data yields roughly order-of-magnitude precision (Table 1). Current force fields can suffer inaccuracies exceeding 1 kcal/mol for free energy *minima*<sup>71-73</sup> and errors at least as large are expected for the barriers which govern kinetics, which have not been part of force field parametrization.<sup>21, 41-42, 74-77</sup> Note for reference that an order of magnitude change in an Arrhenius factor  $\exp(-\Delta G/RT)$  corresponds to a shift in  $\Delta G$  of 1.44 kcal/mol; hence uncertainty of only 0.68 kcal/mol corresponds to a tenfold range.

Accuracy in kinetics also depends on the solvent model. Implicit solvation was employed in the present study, i.e., water molecules were not explicitly modeled. Because such models are in common use,<sup>36, 78-82</sup> it is important to assess their kinetic accuracy. Although the overall computational cost is higher at water-like viscosity ( $\gamma=80 \text{ ps}^{-1}$ ), the estimated average rate constants are found to be only slightly higher to low solvent viscosity ( $\gamma=5 \text{ ps}^{-1}$ ), consistent with prior investigation of the issue.<sup>25</sup> Going forward, additional comparison to explicit-solvent folding rate constants will be an important goal.

Another limitation of the present study is also intrinsic to protein folding generally – namely, ambiguity regarding the unfolded state ensemble. Experimentally, proteins are denatured chemically or with temperature,<sup>83-86</sup> each of which should yield a different unfolded ensemble, and the sensitivity of refolding to the denaturing process is an under-explored topic.<sup>87</sup> Given that some folding times are ms-scale or less, measurements may be sensitive to experimental protocols (e.g., mixing, cooling) occurring on the same timescales. Because of these

ambiguities, we chose to keep our study as controlled as possible and focused specifically on folding from a *single* initial structure, recognizing the importance of future study of ensemble-initialized folding. Our mechanistic discussion above must be seen as restricted to this condition.

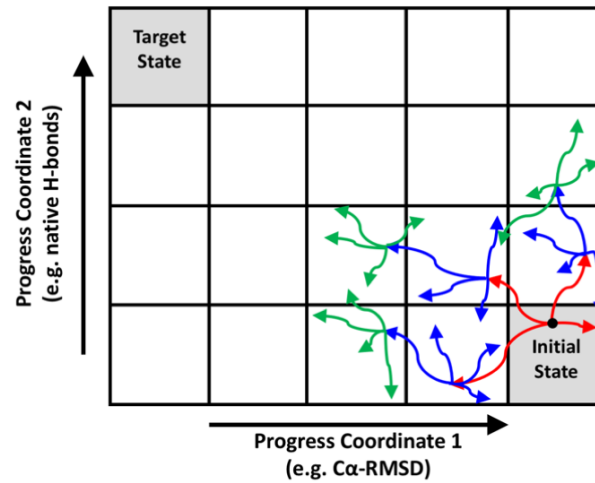
Quantification of statistical uncertainty was a central part of this study, and numerous repeated WE simulations were required to overcome the large variance of the present folding protocol. Although a large variance is generally and rightly a cause for concern in data analysis, our ability to perform tens of truly independent simulations distinguishes this work from typical molecular simulation studies; furthermore, the data presented here exhibited convincingly steady rate estimates. As described elsewhere, neither traditional standard-error analysis nor bootstrapping properly quantify uncertainty in small-size/large-variance data sets.<sup>88</sup> We therefore employed a Bayesian bootstrapping approach which is superior at characterizing precision in such data.<sup>88-89</sup> Nevertheless, no analysis method can correct for insufficient sampling of an unknown distribution, and we estimate that the nominal 95% Bayesian credibility regions reported here empirically correspond to ~60% probability of bracketing the true mean – and such uncertainty in the error analysis is intrinsic to the modest sample sizes.<sup>88</sup> Future studies will clearly benefit from variance-reduction strategies, which have been proposed.<sup>90-91</sup> Lastly, we note that we did *not* perform time averaging (beyond data smoothing over 0.1 or 1 ns windows) so some additional precision gains are possible but they are complicated by time correlations in WE data.<sup>92</sup>

The weighted ensemble method was chosen over other rigorous path sampling approaches<sup>10, 26-30, 46-51</sup> and Markov state models (MSMs).<sup>93-94</sup> Compared to other path sampling methods, WE offers fully scalable parallelization and does not require hard-coding within the dynamics engine in order to “catch” trajectories as they cross interfaces.<sup>33</sup> When compared to MSMs, WE not only avoids any approximation but also offers continuous trajectories and the fine temporal resolution needed to infer mechanistic details occurring on 5-10ns timescales (Figs. S6-S8). By contrast, modern well-validated MSMs often require lag times >100ns.<sup>93-94</sup>

## Acknowledgements

We gratefully acknowledge support from the NIH (Grant GM115805) and from the OHSU Center for Spatial Systems Biomedicine. Computing support was provided by the Center for Research Computing at the University of Pittsburgh. Also, we would like to acknowledge the research effort by Sundar Raman Subramaniam, who performed significant initial simulations on the NTL9 system. Helpful comments on the manuscript were provided by Lillian Chong.

**A**



**B**

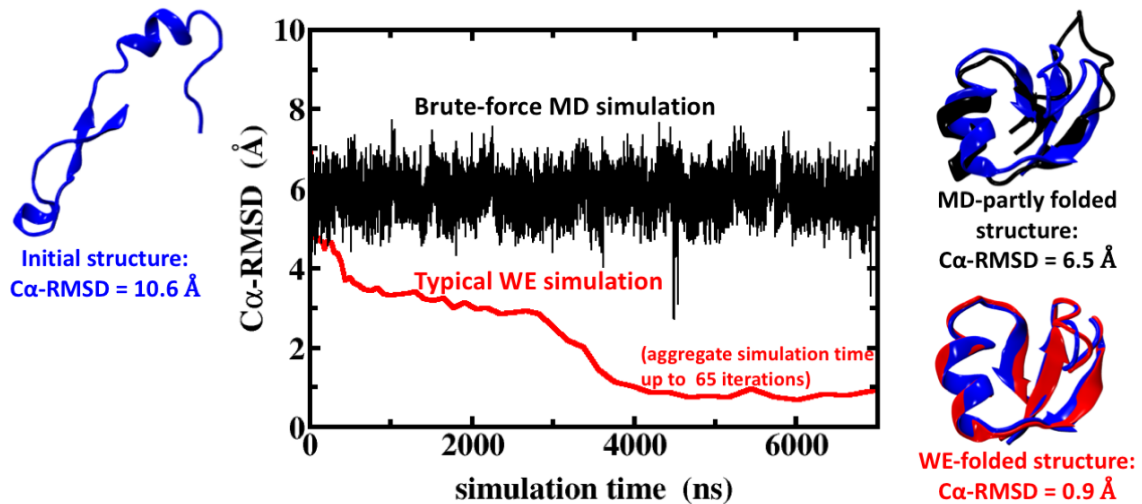
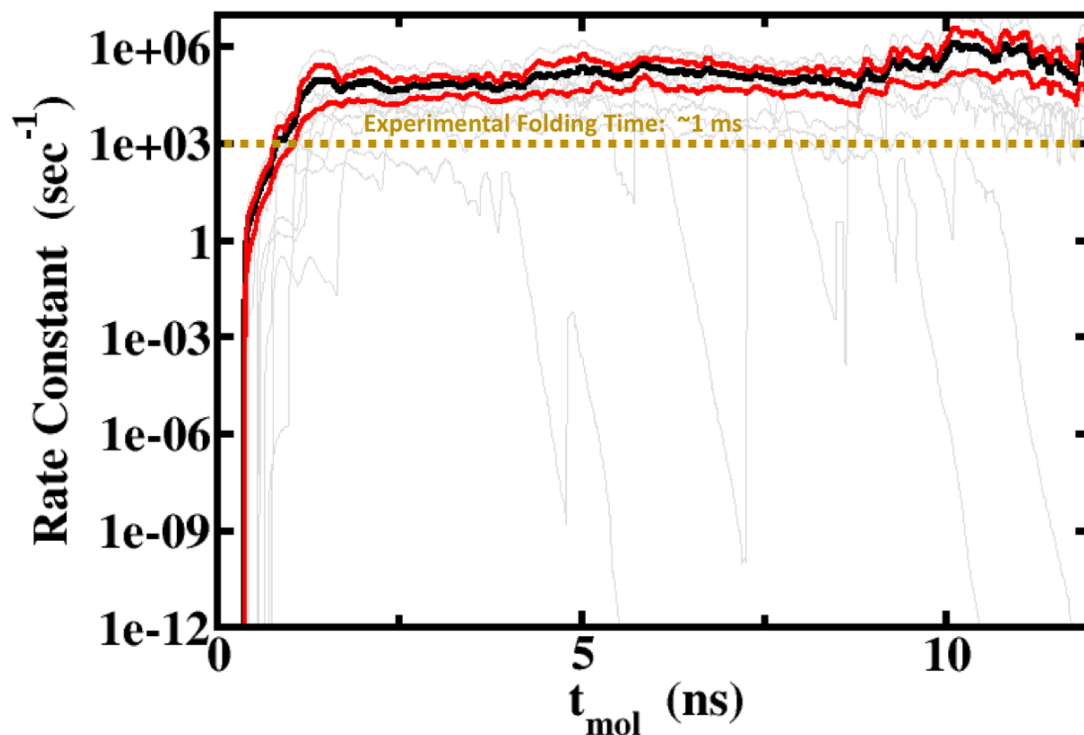


Figure 1: The WE procedure and comparison to regular MD simulation. (A) A schematic of the WE simulation procedure is shown with two-dimensional binning for protein folding. Three iterations (red, then blue, then green) are shown based on a target number of 4 trajectories per bin, illustrating the “statistical ratcheting” effect which is possible without applying biasing forces. Note that a set of new trajectories is shown only for those parent trajectories that reached a new bin. (B) A brute-force MD simulation of NTL9 leads to the “MD-partly folded” structure (black structure) with a C $\alpha$ -RMSD of 6.5 Å with respect to the folded crystal structure (blue structures at right) after 7  $\mu$ s of simulation time. By contrast, a WE simulation starting from the same initial structure (blue structure at left) samples the “WE-folded” NTL9 structure with C $\alpha$ -RMSD < 1 Å (red structure on the right panel). The WE simulation time is the aggregate time including all trajectory segments, representing a fair comparison using roughly the same amount of computational resources.





$C\alpha$ -RMSD = 10.6 Å



$C\alpha$ -RMSD < 1 Å

Figure 2: Evolution of rate constant ( $\text{sec}^{-1}$ ) with molecular time (ns) for NTL9 folding using 2D WE method, with solvent viscosity ( $\gamma$ )  $5 \text{ ps}^{-1}$ . At any molecular time, rate constants were calculated as windowed averages of the previous 100 ps. Gray lines represent individual simulations. The bold black line is the average rate constant from 10 individual simulations, and red lines show the nominal 95% Credibility Region (CR) calculated using the Bayesian bootstrapping.



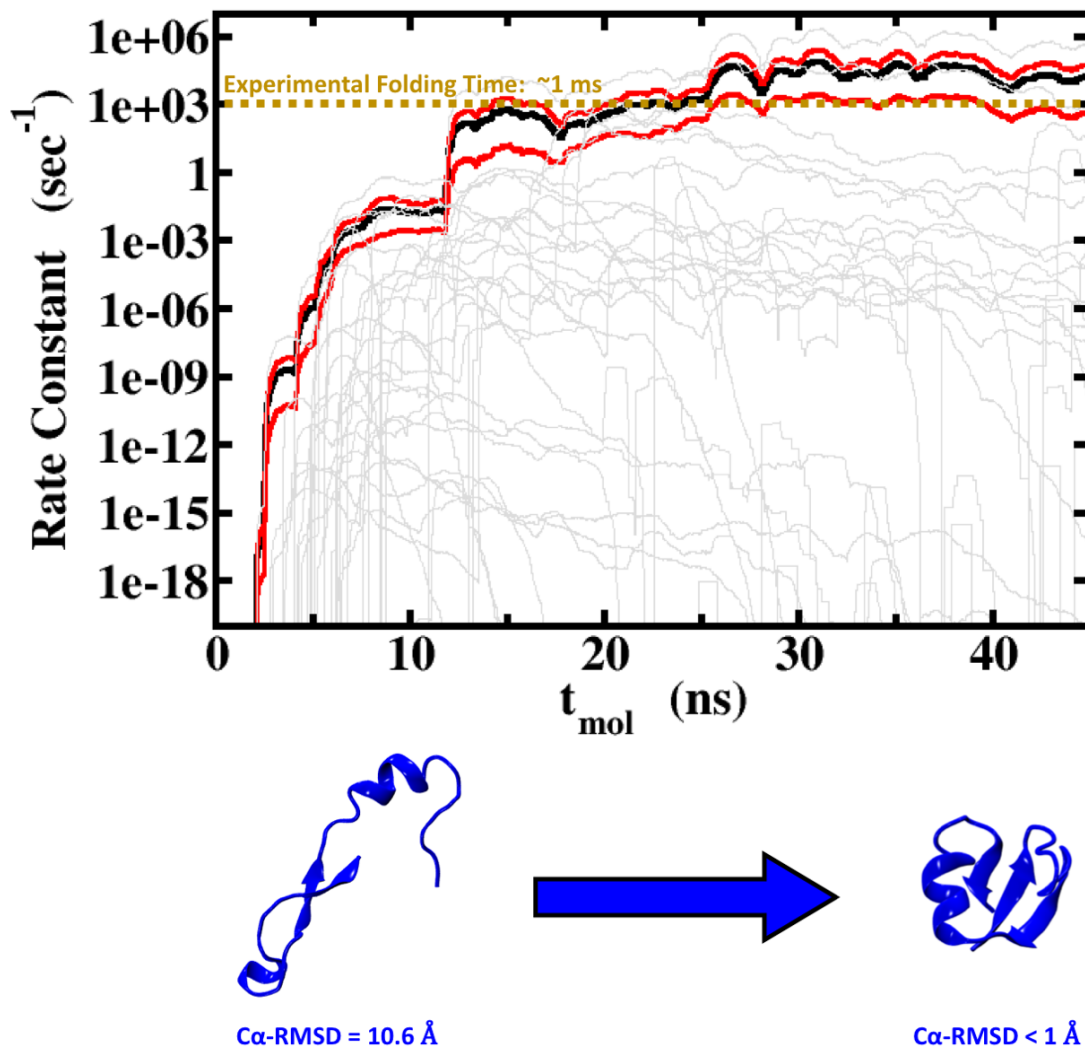


Figure 3: Evolution of rate constant ( $\text{sec}^{-1}$ ) with molecular time (ns) for NTL9 folding using 1D WE method, with solvent viscosity ( $\gamma$ )  $80 \text{ ps}^{-1}$ . At any molecular time, rate constants were calculated as windowed averages of the previous 1000 ps. Gray lines represent individual simulations. The bold black line is the average rate constant from 30 individual simulations, and red lines show the nominal 95% Credibility Region (CR) calculated using the Bayesian bootstrapping.

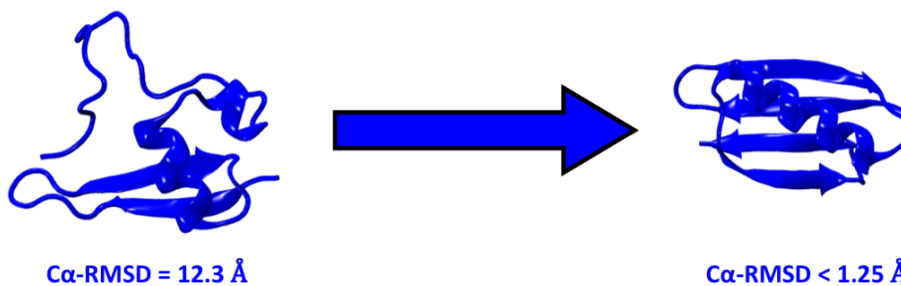
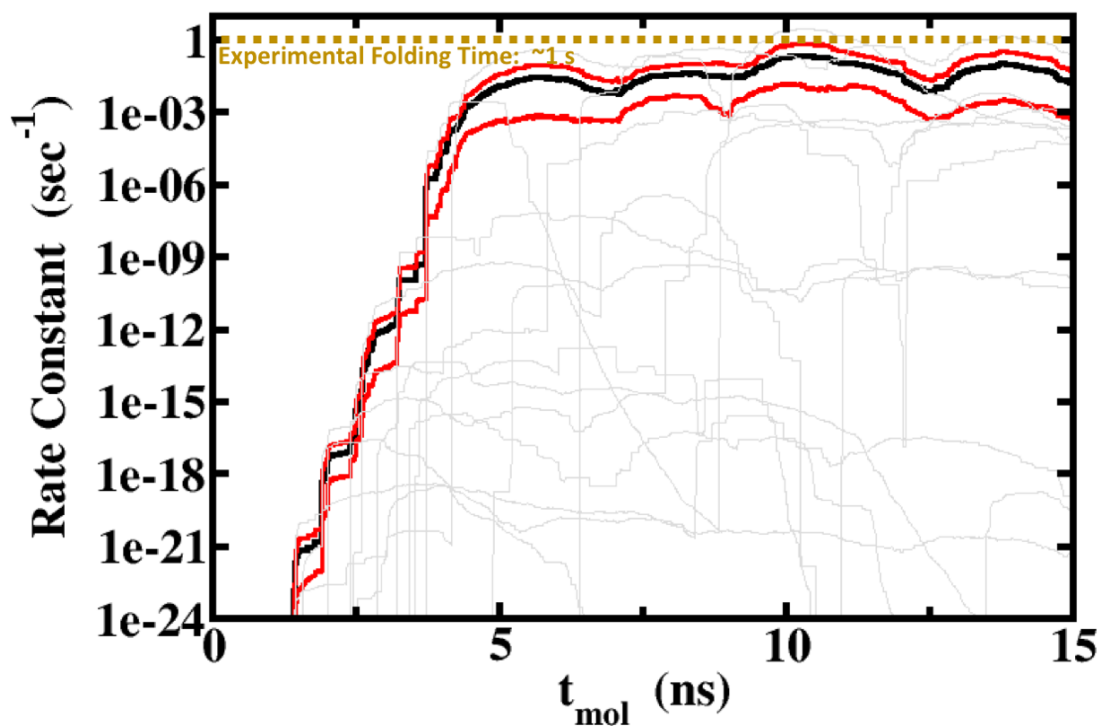


Figure 4: Evolution of rate constant ( $\text{sec}^{-1}$ ) with molecular time (ns) for Protein G folding using 2D WE method, with solvent viscosity ( $\gamma$ )  $5 \text{ ps}^{-1}$ . At any molecular time, rate constants were calculated as windowed averages of the previous 1000 ps. Gray lines represent individual simulations. The bold black line is the average rate constant from 15 individual simulations, and red lines show the nominal 95% Credibility Region (CR) calculated using the Bayesian bootstrapping.

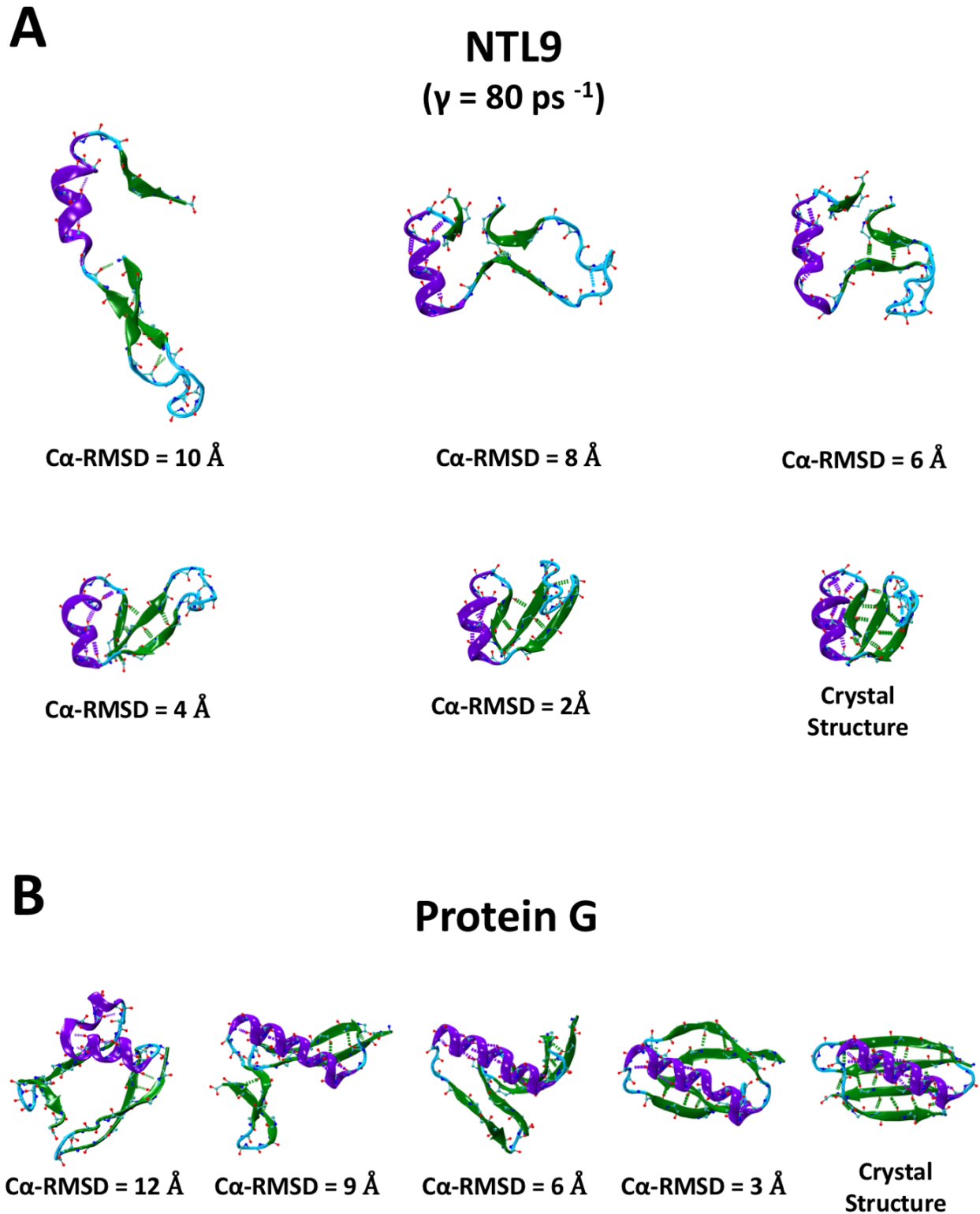


Figure 5: A set of example NTL9 (A) and Protein G (B) structures with decreasing  $C\alpha$ -RMSDs from left to right obtained from a continuous trajectory along with the folded crystal structure. Residues are colored based on their native secondary structures in violet ( $\alpha$ -helix), green ( $\beta$ -

sheet), and cyan (loops). Native backbone hydrogen bonds are indicated as dashed lines, if they emerge in the structure shown.

Table 1: Computational cost and folding rate constants for the three systems studied here (AMBER FF14SB force field).

System	Number of simulations	Molecular time (ns)	Aggregate simulation time ( $\mu$ s)	Wall clock time (days /simulation) (1 GPU card/ $\sim$ 48 CPU cores)	Estimated folding time* [Nominal 95% Credibility Region**]	Experimental folding time
NTL9, $\gamma = 5 \text{ ps}^{-1}$	10	12	115	22	5 $\mu$ s [2 – 12 $\mu$ s]	$\sim$ 1 ms
NTL9, $\gamma = 80 \text{ ps}^{-1}$	30	45	252	20	40 $\mu$ s [16 - 227 $\mu$ s]	$\sim$ 1 ms
Protein G, $\gamma = 5 \text{ ps}^{-1}$	15	15	225	31	19 s [98 – 8 s]	$\sim$ 1 s

\*Averaged from molecular time 2 -12 ns (NTL9,  $\gamma = 5 \text{ ps}^{-1}$ ), 25-45 ns (NTL9,  $\gamma = 80 \text{ ps}^{-1}$ ), and 5-15 ns (Protein G).

\*\* Nominal 95% Bayesian credibility region corresponds to  $\sim$ 60% range of uncertainty: see SI

## References

1. Lindorff-Larsen, K.; Piana, S.; Dror, R. O.; Shaw, D. E., How Fast-Folding Proteins Fold. *Science* **2011**, *334* (6055), 517-520.
2. Englander, S. W.; Mayne, L., The nature of protein folding pathways. *Proceedings of the National Academy of Sciences of the United States of America* **2014**, *111* (45), 15873-80.
3. Wolynes, P. G.; Eaton, W. A., The physics of protein folding. *Physics World* **1999**, *12* (9), 39-44.
4. Go, N., Theoretical Studies of Protein Folding. *Annual Review of Biophysics and Bioengineering* **1983**, *12* (1), 183-210.
5. Bryngelson, J. D.; Wolynes, P. G., Spin glasses and the statistical mechanics of protein folding. *Proceedings of the National Academy of Sciences of the United States of America* **1987**, *84* (21), 7524-8.
6. Matouschek, A.; Kellis, J. T.; Serrano, L.; Fersht, A. R., Mapping the transition state and pathway of protein folding by protein engineering. *Nature* **1989**, *340* (6229), 122-126.
7. Piana, S.; Lindorff-Larsen, K.; Shaw, D. E., Protein folding kinetics and thermodynamics from atomistic simulation. *Proceedings of the National Academy of Sciences of the United States of America* **2012**, *109* (44), 17845-50.
8. Dill, K. A.; MacCallum, J. L., The Protein-Folding Problem, 50 Years On. *Science* **2012**, *338* (6110), 1042-1046.
9. Udgaonkar, J.; Marqusee, S., Folding and binding. *Current Opinion in Structural Biology* **2013**, *23* (1), 1-3.
10. Bolhuis, P. G., Two-state protein folding kinetics through all-atom molecular dynamics based sampling. *Frontiers in bioscience (Landmark edition)* **2009**, *14*, 2801-28.
11. Thirumalai, D.; O'Brien, E. P.; Morrison, G.; Hyeon, C., Theoretical Perspectives on Protein Folding. *Annual Review of Biophysics* **2010**, *39* (1), 159-183.
12. Baker, D.; Agard, D. A., Kinetics versus thermodynamics in protein folding. *Biochemistry* **1994**, *33* (24), 7505-9.
13. Ozkan, S. B.; Dill, K. A.; Bahar, I., Computing the transition state populations in simple protein models. *Biopolymers* **2003**, *68* (1), 35-46.
14. Freddolino, P. L.; Harrison, C. B.; Liu, Y.; Schulten, K., Challenges in protein-folding simulations. *Nature Physics* **2010**, *6* (10), 751-758.
15. Eaton, W. A.; Thompson, P. A.; Chan, C. K.; Hage, S. J.; Hofrichter, J., Fast events in protein folding. *Structure (London, England : 1993)* **1996**, *4* (10), 1133-9.
16. Kubelka, J.; Hofrichter, J.; Eaton, W. A., The protein folding 'speed limit'. *Current Opinion in Structural Biology* **2004**, *14* (1), 76-88.
17. Levitt, M.; Warshel, A., Computer simulation of protein folding. *Nature* **1975**, *253* (5494), 694-8.
18. Rhee, Y. M.; Pande, V. S., Multiplexed-Replica Exchange Molecular Dynamics Method for Protein Folding Simulation. *Biophysical Journal* **2003**, *84* (2), 775-786.
19. Paschek, D.; García, A. E., Reversible Temperature and Pressure Denaturation of a Protein Fragment: A Replica Exchange Molecular Dynamics Simulation Study. *Physical Review Letters* **2004**, *93* (23), 238105-238105.
20. Freddolino, P. L.; Park, S.; Roux, B.; Schulten, K., Force Field Bias in Protein Folding Simulations. *Biophysical Journal* **2009**, *96* (9), 3772-3780.
21. Snow, C. D.; Sorin, E. J.; Rhee, Y. M.; Pande, V. S., How Well Can Simulation Predict Protein Folding Kinetics and Thermodynamics? *Annual Review of Biophysics and Biomolecular Structure* **2005**, *34* (1), 43-69.
22. Dill, K. A.; Ozkan, S. B.; Weikl, T. R.; Chodera, J. D.; Voelz, V. A., The protein folding problem: when will it be solved? *Current Opinion in Structural Biology* **2007**, *17* (3), 342-346.

23. Zwier, M. C.; Chong, L. T., Reaching biological timescales with all-atom molecular dynamics simulations. *Current Opinion in Pharmacology* **2010**, *10* (6), 745-752.
24. Simmerling, C.; Strockbine, B.; Roitberg, A., All-Atom Structure Prediction and Folding Simulations of a Stable Protein. *Journal of the American Chemical Society* **2002**, *124* (38), 11258-11259.
25. Ensign, D. L.; Pande, V. S., Bayesian Single-Exponential Kinetics in Single-Molecule Experiments and Simulations. *The Journal of Physical Chemistry B* **2009**, *113* (36), 12410-12423.
26. Cárdenas, A. E.; Elber, R., Kinetics of cytochrome C folding: Atomically detailed simulations. *Proteins: Structure, Function, and Bioinformatics* **2003**, *51* (2), 245-257.
27. Kuczera, K.; Jas, G. S.; Elber, R., Kinetics of Helix Unfolding: Molecular Dynamics Simulations with Milestoning. *The Journal of Physical Chemistry A* **2009**, *113* (26), 7461-7473.
28. Juraszek, J.; Bolhuis, P. G., Rate Constant and Reaction Coordinate of Trp-Cage Folding in Explicit Water. *Biophysical Journal* **2008**, *95* (9), 4246-4257.
29. Velez-Vega, C.; Borrero, E. E.; Escobedo, F. A., Kinetics and mechanism of the unfolding native-to-loop transition of Trp-cage in explicit solvent via optimized forward flux sampling simulations. *The Journal of Chemical Physics* **2010**, *133* (10), 105103-105103.
30. Borrero, E. E.; Escobedo, F. A., Folding kinetics of a lattice protein via a forward flux sampling approach. *The Journal of Chemical Physics* **2006**, *125* (16), 164904-164904.
31. Huber, G. A.; Kim, S., Weighted-ensemble Brownian dynamics simulations for protein association reactions. *Biophysical Journal* **1996**, *70* (1), 97-110.
32. Chong, L. T.; Saglam, A. S.; Zuckerman, D. M., Path-sampling strategies for simulating rare events in biomolecular systems. *Current Opinion in Structural Biology* **2017**, *43*, 88-94.
33. Zuckerman, D. M.; Chong, L. T., Weighted Ensemble Simulation: Review of Methodology, Applications, and Software. *Annual Review of Biophysics* **2017**, *46* (1), 43-57.
34. Zhang, B. W.; Jasnow, D.; Zuckerman, D. M., The “weighted ensemble” path sampling method is statistically exact for a broad class of stochastic processes and binning procedures. *The Journal of Chemical Physics* **2010**, *132* (5), 054107-054107.
35. Suárez, E.; Pratt, A. J.; Chong, L. T.; Zuckerman, D. M., Estimating first-passage time distributions from weighted ensemble simulations and non-Markovian analyses. *Protein Science* **2016**, *25* (1), 67-78.
36. Voelz, V. A.; Bowman, G. R.; Beauchamp, K.; Pande, V. S., Molecular Simulation of *ab Initio* Protein Folding for a Millisecond Folder NTL9(1–39). *Journal of the American Chemical Society* **2010**, *132* (5), 1526-1528.
37. Fanning, S. W.; Mayne, C. G.; Dharmarajan, V.; Carlson, K. E.; Martin, T. A.; Novick, S. J.; Toy, W.; Green, B.; Panchamukhi, S.; Katzenellenbogen, B. S.; Tajkhorshid, E.; Griffin, P. R.; Shen, Y.; Chandarlapaty, S.; Katzenellenbogen, J. A.; Greene, G. L., Estrogen receptor alpha somatic mutations Y537S and D538G confer breast cancer endocrine resistance by stabilizing the activating function-2 binding conformation. *eLife* **2016**, *5*, e12792-e12792.
38. Speltz, T. E.; Fanning, S. W.; Mayne, C. G.; Fowler, C.; Tajkhorshid, E.; Greene, G. L.; Moore, T. W., Stapled Peptides with  $\gamma$ -Methylated Hydrocarbon Chains for the Estrogen Receptor/Coactivator Interaction. *Angewandte Chemie International Edition* **2016**, *55* (13), 4252-4255.
39. Adelman, Joshua L.; Sheng, Y.; Choe, S.; Abramson, J.; Wright, Ernest M.; Rosenberg, John M.; Grabe, M., Structural Determinants of Water Permeation through the Sodium-Galactose Transporter vSGLT. *Biophysical Journal* **2014**, *106* (6), 1280-1289.
40. Durrant, J. D.; McCammon, J. A., Molecular dynamics simulations and drug discovery. *BMC Biology* **2011**, *9* (1), 71-71.
41. Wang, J.; Wolf, R. M.; Caldwell, J. W.; Kollman, P. A.; Case, D. A., Development and testing of a general amber force field. *Journal of Computational Chemistry* **2004**, *25* (9), 1157-1174.



42. Hornak, V.; Abel, R.; Okur, A.; Strockbine, B.; Roitberg, A.; Simmerling, C., Comparison of multiple Amber force fields and development of improved protein backbone parameters. *Proteins* **2006**, *65* (3), 712-25.
43. Vanommeslaeghe, K.; Hatcher, E.; Acharya, C.; Kundu, S.; Zhong, S.; Shim, J.; Darian, E.; Guvench, O.; Lopes, P.; Vorobyov, I.; Mackerell, A. D., CHARMM general force field: A force field for drug-like molecules compatible with the CHARMM all-atom additive biological force fields. *Journal of Computational Chemistry* **2009**, *31* (4), 671-690.
44. Mackerell, A. D.; Bashford, D.; Bellott, M.; Dunbrack, R. L.; Evanseck, J. D.; Field, M. J.; Fischer, S.; Gao, J.; Guo, H.; Ha, S.; Joseph-McCarthy, D.; Kuchnir, L.; Kuczera, K.; Lau, F. T. K.; Mattos, C.; Michnick, S.; Ngo, T.; Nguyen, D. T.; Prodhom, B.; Reiher, W. E.; Roux, B.; Schlenkrich, M.; Smith, J. C.; Stote, R.; Straub, J.; Watanabe, M.; Wiórkiewicz-Kuczera, J.; Yin, D.; Karplus, M., All-Atom Empirical Potential for Molecular Modeling and Dynamics Studies of Proteins *The Journal of Physical Chemistry B* **1998**, *102* (18), 3586-3616.
45. William, L. J.; David S. Maxwell, A.; Tirado-Rives, J., Development and Testing of the OPLS All-Atom Force Field on Conformational Energetics and Properties of Organic Liquids. *J. Am. Chem. Soc.* **1996**, *118* (45), 11225-11236.
46. Bolhuis, P. G.; Chandler, D.; Dellago, C.; Geissler, P. L., Transition Path Sampling: Throwing Ropes Over Rough Mountain Passes, in the Dark. *Annual Review of Physical Chemistry* **2002**, *53* (1), 291-318.
47. van Erp, T. S.; Moroni, D.; Bolhuis, P. G., A novel path sampling method for the calculation of rate constants. *The Journal of Chemical Physics* **2003**, *118* (17), 7762-7774.
48. Allen, R. J.; Warren, P. B.; ten Wolde, P. R., Sampling Rare Switching Events in Biochemical Networks. *Physical Review Letters* **2005**, *94* (1), 018104-018104.
49. Warmflash, A.; Bhimalapuram, P.; Dinner, A. R., Umbrella sampling for nonequilibrium processes. *The Journal of Chemical Physics* **2007**, *127* (15), 154112-154112.
50. Faradjian, A. K.; Elber, R., Computing time scales from reaction coordinates by milestoning. *The Journal of Chemical Physics* **2004**, *120* (23), 10880-10889.
51. Bello-Rivas, J. M.; Elber, R., Exact milestoning. *The Journal of Chemical Physics* **2015**, *142* (9), 094102-094102.
52. Nunes-Alves, A.; Zuckerman, D. M.; Arantes, G. M., Escape of a Small Molecule from Inside T4 Lysozyme by Multiple Pathways. *Biophysical Journal* **2018**, *114* (5), 1058-1066.
53. Donovan, R. M.; Tapia, J.-J.; Sullivan, D. P.; Faeder, J. R.; Murphy, R. F.; Dittrich, M.; Zuckerman, D. M., Unbiased Rare Event Sampling in Spatial Stochastic Systems Biology Models Using a Weighted Ensemble of Trajectories. *PLOS Computational Biology* **2016**, *12* (2), e1004611-e1004611.
54. Donovan, R. M.; Sedgewick, A. J.; Faeder, J. R.; Zuckerman, D. M., Efficient stochastic simulation of chemical kinetics networks using a weighted ensemble of trajectories. *The Journal of Chemical Physics* **2013**, *139* (11), 115105.
55. Suárez, E.; Lettieri, S.; Zwier, M. C.; Stringer, C. A.; Subramanian, S. R.; Chong, L. T.; Zuckerman, D. M., Simultaneous Computation of Dynamical and Equilibrium Information Using a Weighted Ensemble of Trajectories. *Journal of Chemical Theory and Computation* **2014**, *10* (7), 2658-2667.
56. Adelman, Joshua L.; Dale, Amy L.; Zwier, Matthew C.; Bhatt, D.; Chong, Lillian T.; Zuckerman, Daniel M.; Grabe, M., Simulations of the Alternating Access Mechanism of the Sodium Symporter Mhp1. *Biophysical Journal* **2011**, *101* (10), 2399-2407.
57. Zwier, M. C.; Pratt, A. J.; Adelman, J. L.; Kaus, J. W.; Zuckerman, D. M.; Chong, L. T., Efficient Atomistic Simulation of Pathways and Calculation of Rate Constants for a Protein–Peptide Binding Process: Application to the MDM2 Protein and an Intrinsically Disordered p53 Peptide. *The Journal of Physical Chemistry Letters* **2016**, *7* (17), 3440-3445.



58. Saglam, A. S.; Wang, D. W.; Zwier, M. C.; Chong, L. T., Flexibility vs Preorganization: Direct Comparison of Binding Kinetics for a Disordered Peptide and Its Exact Preorganized Analogues. *The Journal of Physical Chemistry B* **2017**, *121* (43), 10046-10054.
59. Zwier, M. C.; Adelman, J. L.; Kaus, J. W.; Pratt, A. J.; Wong, K. F.; Rego, N. B.; Suárez, E.; Lettieri, S.; Wang, D. W.; Grabe, M.; Zuckerman, D. M.; Chong, L. T., WESTPA: An Interoperable, Highly Scalable Software Package for Weighted Ensemble Simulation and Analysis. *Journal of Chemical Theory and Computation* **2015**, *11* (2), 800-809.
60. Pearlman, D. A.; Case, D. A.; Caldwell, J. W.; Ross, W. S.; Cheatham, T. E.; DeBolt, S.; Ferguson, D.; Seibel, G.; Kollman, P., AMBER, a package of computer programs for applying molecular mechanics, normal mode analysis, molecular dynamics and free energy calculations to simulate the structural and energetic properties of molecules. *Computer Physics Communications* **1995**, *91* (1-3), 1-41.
61. Case, D. A.; Cheatham, T. E.; Darden, T.; Gohlke, H.; Luo, R.; Merz, K. M.; Onufriev, A.; Simmerling, C.; Wang, B.; Woods, R. J.; Wang, B.; Woods, R. J., The Amber biomolecular simulation programs. *Journal of computational chemistry* **2005**, *26* (16), 1668-88.
62. Case, D. A., Cerutti, D. S., Cheatham III, T. E., Darden, T. A., Duke, R. E., Giese, T. J., Gohlke, H., Goetz, A. W., Greene, D., Homeyer, N., Izadi, S., Kovalenko, A., Lee, T. S., LeGrand, S., Li, P., Lin, C., Liu, J., Luchko, T., Luo, R., Mermelstein, D., Merz, K. M., Monard, G., York, H. D. M., Kollman, P. A., Amber 2017, University of California, San Francisco. **2017**.
63. Hill, T. L., State Probabilities and Fluxes in Terms of the Rate Constants of the Diagram. Springer New York: New York, NY, 1989; pp 39-88.
64. Feig, M., Kinetics from Implicit Solvent Simulations of Biomolecules as a Function of Viscosity. *J Chem Theory Comput* **2007**, *3* (5), 1734-1748.
65. Anandakrishnan, R.; Drozdetski, A.; Walker, Ross C.; Onufriev, Alexey V., Speed of Conformational Change: Comparing Explicit and Implicit Solvent Molecular Dynamics Simulations. *Biophysical Journal* **2015**, *108* (5), 1153-1164.
66. Zagrovic, B.; Pande, V., Solvent viscosity dependence of the folding rate of a small protein: Distributed computing study. *Journal of Computational Chemistry* **2003**, *24* (12), 1432-1436.
67. Shaw, D. E.; Maragakis, P.; Lindorff-Larsen, K.; Piana, S.; Dror, R. O.; Eastwood, M. P.; Bank, J. A.; Jumper, J. M.; Salmon, J. K.; Shan, Y.; Wriggers, W., Atomic-level characterization of the structural dynamics of proteins. *Science (New York, N.Y.)* **2010**, *330* (6002), 341-6.
68. Chung, H. S.; McHale, K.; Louis, J. M.; Eaton, W. A., Single-Molecule Fluorescence Experiments Determine Protein Folding Transition Path Times. *Science* **2012**, *335* (6071), 981-984.
69. Zuckerman, D. M.; Woolf, T. B., Transition events in butane simulations: Similarities across models. *The Journal of Chemical Physics* **2002**, *116* (6), 2586.
70. Zhang, B. W.; Jasnow, D.; Zuckerman, D. M., Transition-event durations in one-dimensional activated processes. *The Journal of Chemical Physics* **2007**, *126* (7), 074504.
71. Shirts, M. R.; Pitera, J. W.; Swope, W. C.; Pande, V. S., Extremely precise free energy calculations of amino acid side chain analogs: Comparison of common molecular mechanics force fields for proteins. *The Journal of Chemical Physics* **2003**, *119* (11), 5740-5761.
72. Fujitani, H.; Tanida, Y.; Ito, M.; Jayachandran, G.; Snow, C. D.; Shirts, M. R.; Sorin, E. J.; Pande, V. S., Direct calculation of the binding free energies of FKBP ligands. *The Journal of Chemical Physics* **2005**, *123* (8), 084108-084108.
73. Shirts, M. R.; Mobley, D. L.; And, J. D. C.; Pande, V. S., Accurate and Efficient Corrections for Missing Dispersion Interactions in Molecular Simulations. *J. Phys. Chem. B* **2007**, *111* (45), 13052-13063.
74. Wang, L.-P.; Martinez, T. J.; Pande, V. S., Building Force Fields: An Automatic, Systematic, and Reproducible Approach. *The Journal of Physical Chemistry Letters* **2014**, *5* (11), 1885-1891.

75. Beauchamp, K. A.; Lin, Y.-S.; Das, R.; Pande, V. S., Are Protein Force Fields Getting Better? A Systematic Benchmark on 524 Diverse NMR Measurements. *Journal of Chemical Theory and Computation* **2012**, *8* (4), 1409-1414.
76. Debiec, K. T.; Cerutti, D. S.; Baker, L. R.; Gronenborn, A. M.; Case, D. A.; Chong, L. T., Further along the Road Less Traveled: AMBER ff15ipq, an Original Protein Force Field Built on a Self-Consistent Physical Model. *Journal of Chemical Theory and Computation* **2016**, *12* (8), 3926-3947.
77. Maier, J. A.; Martinez, C.; Kasavajhala, K.; Wickstrom, L.; Hauser, K. E.; Simmerling, C., ff14SB: Improving the Accuracy of Protein Side Chain and Backbone Parameters from ff99SB. *Journal of Chemical Theory and Computation* **2015**, *11* (8), 3696-3713.
78. Hua, D. P.; Huang, H.; Roy, A.; Post, C. B., Evaluating the dynamics and electrostatic interactions of folded proteins in implicit solvents. *Protein Science* **2016**, *25* (1), 204-218.
79. Cumberworth, A.; Bui, J. M.; Gsponer, J., Free energies of solvation in the context of protein folding: Implications for implicit and explicit solvent models. *Journal of Computational Chemistry* **2016**, *37* (7), 629-640.
80. Shao, Q.; Zhu, W., Assessing AMBER force fields for protein folding in an implicit solvent. *Physical chemistry chemical physics : PCCP* **2018**, *20* (10), 7206-7216.
81. Nguyen, H.; Pérez, A.; Bermeo, S.; Simmerling, C., Refinement of Generalized Born Implicit Solvation Parameters for Nucleic Acids and Their Complexes with Proteins. *Journal of Chemical Theory and Computation* **2015**, *11* (8), 3714-3728.
82. Nguyen, H.; Maier, J.; Huang, H.; Perrone, V.; Simmerling, C., Folding Simulations for Proteins with Diverse Topologies Are Accessible in Days with a Physics-Based Force Field and Implicit Solvent. *Journal of the American Chemical Society* **2014**, *136* (40), 13959-13962.
83. Kuhlman, B.; Luisi, D. L.; Evans, P. A.; Raleigh, D. P., Global analysis of the effects of temperature and denaturant on the folding and unfolding kinetics of the N-terminal domain of the protein L9. *Journal of Molecular Biology* **1998**, *284* (5), 1661-1670.
84. Möglich, A.; Krieger, F.; Kiefhaber, T., Molecular Basis for the Effect of Urea and Guanidinium Chloride on the Dynamics of Unfolded Polypeptide Chains. *Journal of Molecular Biology* **2005**, *345* (1), 153-162.
85. Taskent, H.; Cho, J.-H.; Raleigh, D. P., Temperature-Dependent Hammond Behavior in a Protein-Folding Reaction: Analysis of Transition-State Movement and Ground-State Effects. *Journal of Molecular Biology* **2008**, *378* (3), 699-706.
86. Burcu Anil; Ying Li; Jae-Hyun Cho; Raleigh, D. P., The Unfolded State of NTL9 Is Compact in the Absence of Denaturant. **2006**.
87. Guinn, E. J.; Marqusee, S., Exploring the Denatured State Ensemble by Single-Molecule Chemo-Mechanical Unfolding: The Effect of Force, Temperature, and Urea. *Journal of Molecular Biology* **2018**, *430* (4), 450-464.
88. Mostofian, B.; Zuckerman, D. M., Error analysis for small-sample, high-variance data: Cautions for bootstrapping and Bayesian bootstrapping. *arXiv:1806.01998* **2018**, 1-15.
89. Rubin, D. B., The Bayesian Bootstrap. *The Annals of Statistics* **1981**, *9* (1), 130-134.
90. Aristoff, D., Analysis and optimization of weighted ensemble sampling. *ESAIM: Mathematical Modelling and Numerical Analysis* **2017**, <https://doi.org/10.1051/m2an/2017046>-<https://doi.org/10.1051/m2an/2017046>.
91. Aristoff, D.; Zuckerman, D. M., Optimizing Weighted Ensemble Sampling of Steady States. *arXiv:1806.00860* **2018**, 1-19.
92. Zhang, B. W.; Jasnow, D.; Zuckerman, D. M., Efficient and verified simulation of a path ensemble for conformational change in a united-residue model of calmodulin. *Proceedings of the National Academy of Sciences* **2007**, *104* (46), 18043-18048.

93. Lane, T. J.; Bowman, G. R.; Beauchamp, K.; Voelz, Vincent A.; Pande, V., Markov State Model Reveals Folding and Functional Dynamics in Ultra-Long MD Trajectories. *Journal of the American Chemical Society* **2011**, *133* (45), 18413-18419.
94. Schwantes, C. R.; Pande, V. S., Improvements in Markov State Model Construction Reveal Many Non-Native Interactions in the Folding of NTL9. *Journal of Chemical Theory and Computation* **2013**, *9* (4), 2000-2009.